

Two-Photon Polymerization of a Branched Hollow Fiber Structure with predefined Circular Pores

Matthias Bieda^a, Felix Bouchard^{a, b, 1}, Andrés F. Lasagni^{a, b}

^a Fraunhofer-Institut für Werkstoff- und Strahltechnik (IWS), Winterbergstr. 28, 01277 Dresden, Germany

^b Technische Universität Dresden, Institut für Fertigungstechnik, 01062 Dresden, Germany

Corresponding author:

Matthias Bieda

Fraunhofer-Institut für Werkstoff- und Strahltechnik IWS

Winterbergstraße 28, 01277 Dresden, Germany

Phone: (+) 49 (0)351/833913348

Email: matthias.bieda@iws.fraunhofer.de

matthias.bieda@iws.fraunhofer.de

Keywords: Two-Photon Polymerization, Microfluidic, Porous Hollow Fiber, 3D Microfabrication

Abstract

Porous fiber structures are of great concern to many fields of life-science engineering, but require a complex assembly processes that have geometric constraints. For this reason, tremendous efforts were expended in recent years to develop micro-/nano fabrication techniques. We report on the 3D structuring of a 3.5 mm long branched hollow fiber with 150 μm outer diameter and predefined circular pores (diameter: 30 μm). The investigated process is based on two-photon polymerization (2PP) of the UV curing resin OrmoComp®. The incident light of a femtosecond pulsed laser at 790 nm wavelength is used to generate the structure. Utilizing the non-linear behavior of two-photon absorption due to a tightly focused, high-intensity laser beam allows the local fabrication of three-dimensional structures in the photoresist. Voxels fabricated by 2PP are studied by controlling average laser power and exposure time. The appropriate average pulse energy and writing speed are determined to apply the optimal exposure parameters concerning the geometric accuracy and overall quality of the structure. The 2PP direct laser writing process is employed to generate the hollow fiber at an average laser power of 105 mW, and a writing speed of 5.0 mm/s. Water flowing through the fiber provides evidence that the core is hollow.

1. Introduction

Two-photon polymerization (2PP) is a three-dimensional microfabrication method that typically uses a near-infrared femtosecond laser source to generate polymeric structures. This technology has already been employed to fabricate biocompatible structures for cell cultures [1 - 9], micro-optics on optical fibers [10] and surface plasmon polaritons [11], microscale medical devices [12, 13], nano-/micro electrodes [14], and micro-cantilevers [15].

The simultaneous absorption of two or more photons by an atom or molecule was first predicted in 1931 by Göppert-Mayer [16]. It took 30 years until Kaiser and Garrett used a ruby optical maser to illuminate $\text{CaF}_2:\text{Eu}^{2+}$ crystals, providing practical confirmation of two-photon excitation [17]. Since then, studies in the area of two photon processes have increased greatly, owing to the commercial availability of high power ultra-short-pulse-width lasers. Because of the high photon intensities required to initiate two-photon absorption (2PA), femtosecond lasers are commonly employed in two photon processes. A comprehensive review introducing both the theoretical framework and applications of 2PP is given, for example, in Ref. [18], [19] and [20].

¹ Present address: CREA VAC GmbH, Löbtauer Str. 65-71, 01159 Dresden, Germany

On the basis of 2PP, the fabrication of a branched hollow fiber with predefined pores is demonstrated. Branched hollow fibers are common in nature, but it is still a challenge to generate such artificial structures. These fibers can potentially be used in microfluidics, artificial blood vessels, and tissue engineering. Processing methods used in the past to produce alginate or hydrogel based hollow fibers were based on microfluidic chips [21], micro-nozzle devices [22], and weaving systems [23]. A multi-porous hollow fiber was fabricated using a solvent-system combined with an electrospinning process [24]. However, these multi-step methods have geometry constraints and design limitations. The advantageous ability to generate capillary feature sizes in the sub-micro-meter range shows the potential of 2PP to produce hollow fibers, and opens up an unprecedented flexibility in 3D design compared to other technologies. Hollow fibers with predetermined pores of different sizes and shapes can also be easily realized, enabling an adequate supply of nutrients to cells, for example, in an *in-vitro* microfluidic environment.

Employing 2PP to create microfluidic channels was demonstrated in the past. For example, large-area masked multiphoton absorption polymerization was used to produce channels with rectangular cross-section in Fluor-SU-8, a specially mixed formulation of the commercially available SU-8 resin [25]. Also, fluidic channels with circular cross-sections were fabricated [26, 27]. However, these techniques require either extensive preparation of the resin or present rather simple single channel geometry in the micrometer scale which are inherently difficult to integrate in a lab-on-a-chip system, for example. This study presents an approach for generating a millimeter long porous branched hollow fiber by adopting 2PP as a real 3D fabrication process. With regard to the fabrication process, the minimum lateral and spatial resolution of the polymerized focal volume are investigated using the ascending scan method [28]. The voxel size of the polymerized material is determined as a function of exposure time and laser power in order to identify appropriate process parameters, which are necessary to fabricate mechanically stable structures. Without knowing the accurate overlapping of the voxels, it would not be possible to produce the desired 3D geometry.

2. Materials and Methods

2.1 Material preparation

The commercially available UV curing photoresist OrmoComp®, supplied by micro resist Technology GmbH, is a brand name of Ormocer, an organic-inorganic hybrid material, which was proven to be very suitable for two- and three-photon polymerization in previous studies [11, 29]. The basic molecular components are the cross-linker Trimethylolpropantriacylat (TMPTA) and the reactive diluent 3-(Mercaptopropyl) methylmethoxysilane (MMS). It was chosen for this investigation, because it already contains the photoinitiator Diphenyl (2, 4, 6 - trimethylbenzoyl) phosphine oxide (Lucirin® TPO-L) [30]. However, the concentration of the photoinitiator is not provided by the supplier.

A drop (ca. 10 μ l) of OrmoComp® was placed between a 1 mm thick Superfrost® microscope slide of 76 x 26 mm² (Carl Roth GmbH & Co. KG) and a glass coverslip (24 x 60 mm², thickness: 170 \pm 5 μ m) which were separated by glass spacers (18 x 18 mm²) with a thickness of 170 \pm 5 μ m and dried on a hot plate at 80°C for 60 seconds (Fig. 1a). In order to fabricate large structures, two spacers with a total thickness of 340 \pm 10 μ m were placed on top of each other. After the laser exposure, the samples were post-baked at 130°C for 10 minutes to improve adhesion between the object glass and the polymerized material, and finally immersed in a Petri dish (diameter: 90 mm) filled with the commercially available developer OrmoDev (micro resist technology GmbH) for approximately 10 minutes to wash away any unsolidified resist. The samples were always completely covered by the developer solution. The volume shrinkage of the photoresist during cure is approximately 5 – 7% according to the material data sheet which is given by the supplier. Low shrinkage is necessary both to minimize stress and provide long term stability.

2.2 Experimental setup

A scheme for the experimental setup of the 2PP fabrication method is shown in Fig. 1b. The excitation source is a mode-locked Ti:Sapphire laser (femtoTrain 500, High Q Laser GmbH), which produces pulses with a duration of 72 fs at a wavelength of 790 nm at the laser output. It has to be mentioned, though, that the pulse length is increased when the laser radiation passes through different transmissive elements (in our case, through a beam expander and a focus objective). This can reduce the sensitivity of the 2PA technique since the intensity of the pulse at the focus decreases. The repetition frequency of the laser is 73 MHz and the maximum average power 500 mW. A rotatable half-wave-plate (HWP) in combination with a polarizing beam splitter was used to control the laser output power. An acousto-optic modulator (AOM, MT110 by AA Opto-Electronic) was used as a shutter to release or block the laser beam, respectively. The beam was expanded to overfill the objective's entrance aperture to reduce the spot size. The diameter of the incoming beam was 8 mm. The beam enters a dichroic mirror and is directed into a focus objective (Planapochromat 20x/0.8 M27, Carl Zeiss GmbH) with 20x magnification and a Numerical Aperture (NA) of 0.8, which is attached to an air-bearing Z-stage (ABL10050, Aerotech Inc., max. distance: 100 mm). The sample is mounted on computer controlled high-resolution air-bearing XY-stages (ABL15010, Aerotech Inc., max. distance: 100 mm), and can therefore be moved in three dimensions relative to the focus of the laser beam. A light source (LED at 630 nm) is used to view the sample with a CCD camera, ensuring proper positioning and monitoring the process in real time.

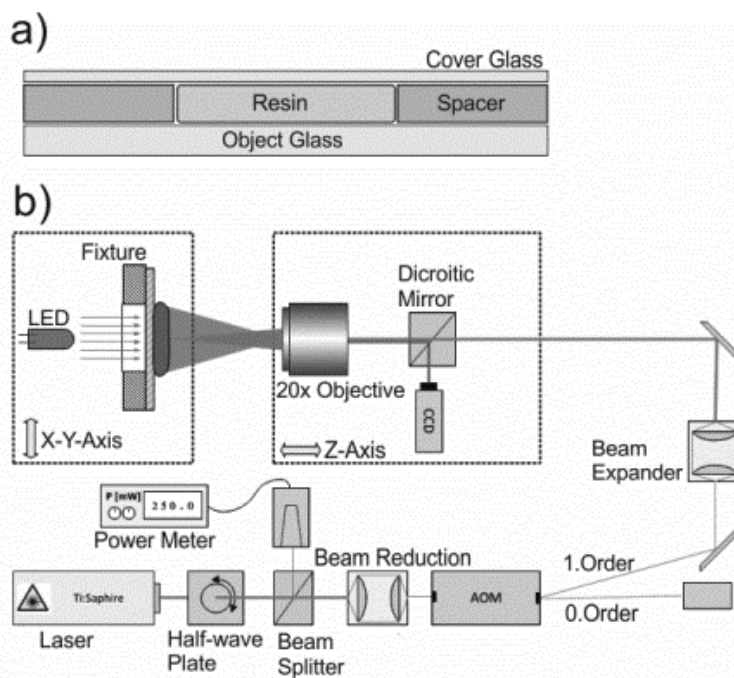


Figure 1: a) Sample layout used for the 2PP experiments; b) Schematic of the experimental setup for the 2PP experiments.

3. Results and Discussion

3.1 Minimal achievable resolution on OrmoComp® with a 20x (NA = 0.8) objective

The minimal achievable resolution of a 2PP process is given by the voxel size. A voxel is a single volume element created by point-to-point exposure with a certain length and width. For the investigated OrmoComp® photoresist, both axial (length) and lateral resolution (width) of such an isolated polymerized element depend on average laser power (P_{avg}) and exposure time (τ_{exp}). The voxel size is crucial to the success of the microfabrication process since it determines the accuracy to the position of a pre-existing element. Figure 2 shows the experimental approach (Fig. 2a) and the individual voxels (Fig. 2b). 2PP was employed to generate these isolated voxels with repeated re-focusing the beam. The focus positions were chosen to ensure that the voxels attach to the cover glass after development.

At the first position, the exposure volume was completely buried in glass, and no material was exposed (Fig. 2a). The voxels were separated by 10 μm in the lateral direction, while the focal position in the vertical direction varied 0.75 μm / step. Width and length of the dropped voxels, which were still attached to the cover glass, were measured from SEM images. Figure 2b shows an example of voxels for the OrmoComp® photoresist that were exposed at an average power between 37.3 mW and 148.1 mW (measured at the back aperture of the objective). For each power, a constant exposure time of 20 ms was used. Every row shows the voxels for one specific power, e.g. 148.1 mW (row 1). As shown in Fig. 2b, voxels on the left of the rows are focused the deepest in the glass and are barely visible. Voxels on the right of the row fell onto the cover glass because they were too shallow to remain attached to the cover glass.

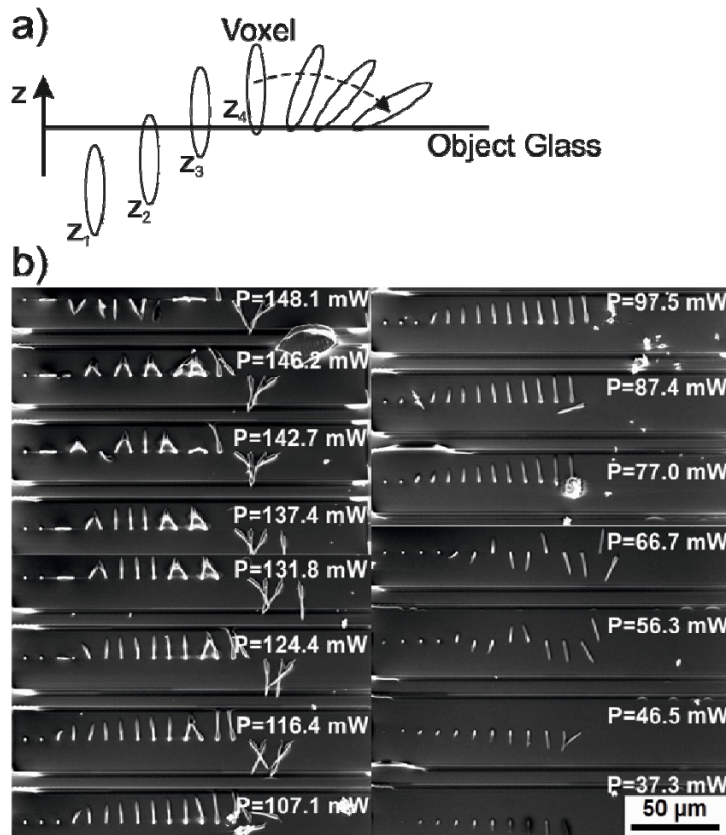


Figure 2: (a) Schematic of the conducted experiments to determine the voxel size as function of exposure time and average power (z : position of the laser focus); (b) Voxels along the glass substrate with $P_{avg} = 37.3 - 148.1$ mW at different focus positions (exposure time: $\tau_{exp} = 20$ ms)

Figure 3 depicts width and length of the generated voxels as function of different laser power and exposure times. It can be observed that voxel growth deviates from a linear exposure behavior. The shape of voxels created by 2PP varies from highly elongated ellipsoids to more imperfect spheres depending on average laser power and exposure time. A tendency to larger voxels is predominantly observed for higher laser power, and longer exposure time. The increase of the voxel width was from 0.6 μm ($\tau_{exp} = 0.01$ ms, $P_{avg} = 55$ mW) to 4.9 μm ($\tau_{exp} = 100$ ms, $P_{avg} = 145$ mW). The voxel length varied between 2.6 μm ($\tau_{exp} = 0.01$ ms, $P_{avg} = 55$ mW) and 37.6 μm ($\tau_{exp} = 100$ ms, $P_{avg} = 145$ mW). The minimal lateral voxel size was 0.6 μm , while the according longitudinal resolution is 2.6 μm .

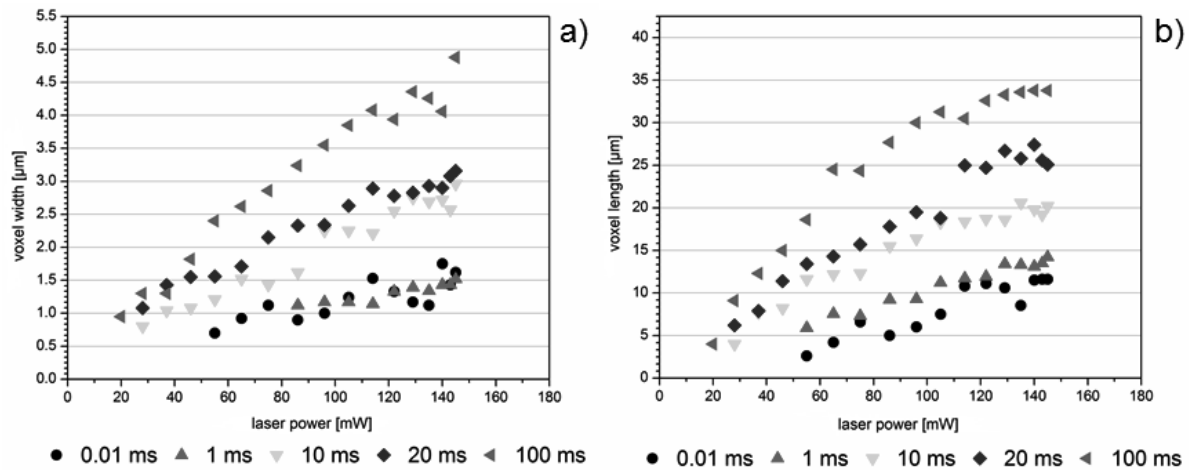


Figure 3: (a) Voxel width and (b) length in OrmoComp® for different laser power ($P_{avg} = 20$ to 150 mW) and exposure times ($\tau_{exp} = 0.01$ to 100 ms).

3.2 Evaluation of structure quality as function of writing speed and laser power

Lattice structures were written via 2PP to determine the maximum feasible writing speed in OrmoComp® (see Fig. 4). The writing speed was varied between 0.1 and 11 mm/s, while the average laser power was set between 28 and 145 mW. The lattice structures had a total size of 100 μm x 100 μm with a 10 μm separated inner structure (10 by 10 cells). A schematic layout of the performed analysis and its results can be observed in Fig. 4a. Scanning Electron Microscopy analysis of the lattice structures revealed the threshold behavior of the 2PP process (Fig. 4b - 4d). The polymerization threshold is defined as the level of laser intensity where the photochemical reaction becomes irreversible. Hence, the ability to fabricate the lattice in Fig. 4b - 4d depends greatly on the ratio of laser power and writing speed.

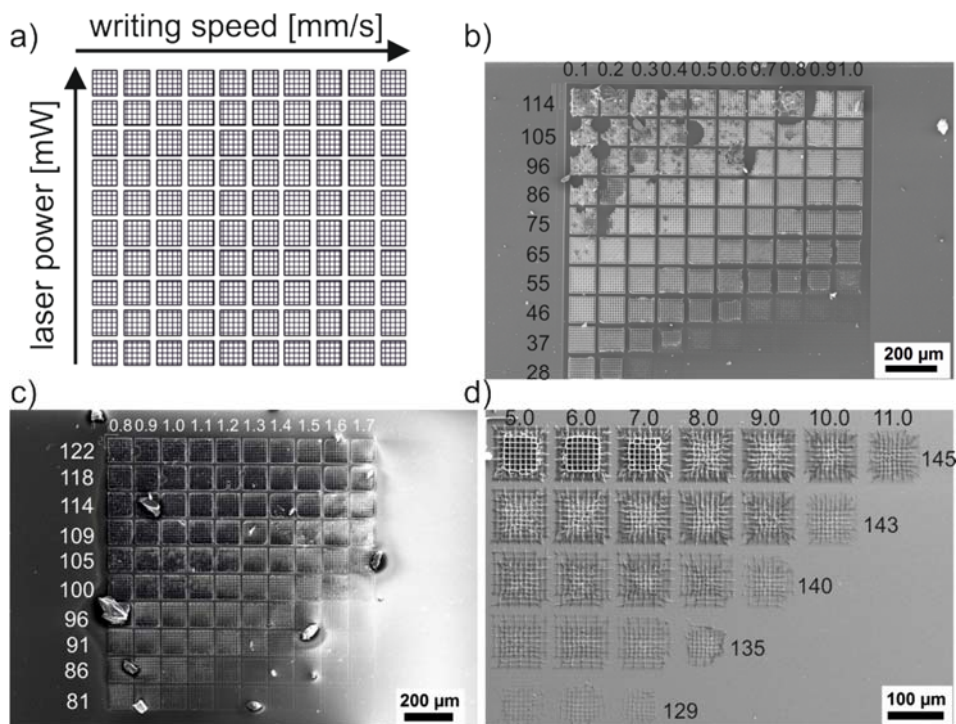


Figure 4: Evaluation matrix of lattice structures to determine the processing parameters for the 2PP process: a) Schematic layout with the values of writing speed (horizontal axis) and laser power (vertical axis); SEM image for b) 0.1 – 1.0 mm/s writing speed and 28 – 114 mW laser power; c) 0.8 – 1.7 mm/s writing speed and 81 – 122 mW laser power; d) 5.0 – 11.0 mm/s writing speed and 129 – 145 mW laser power.

Different parameter combinations (laser power vs. writing speed) led to a difference in the amount of polymer crosslinking, producing material with different mechanical properties (Fig. 5). Uniform structures without defects are possible by adjusting the laser power just slightly above the threshold. The initially designed straight features are maintained (Fig. 5a). It also does not exhibit significant shrinkage upon cure. However, lattices produced with improper parameters can show signs of distortion due to the solvent used to wash away the non-polymerized material (Fig. 5b – 5d). By increasing the writing speed at constant laser power, minor non-polymerized lattice structures showed unstable edges (Fig. 5b). This effect can be explained by a poor attachment of the near-edge lines due to a mismatch of laser power and writing speed at the beginning of each line. If the laser intensity is above the damage threshold, the irradiated material can be boiled away (Fig. 5c). No polymerization occurred for lattices fabricated with low laser power and/or high writing speeds. In the last case, the cumulated energy is lower than the laser intensity which is needed to initiate a polymerization reaction (Fig. 5d).

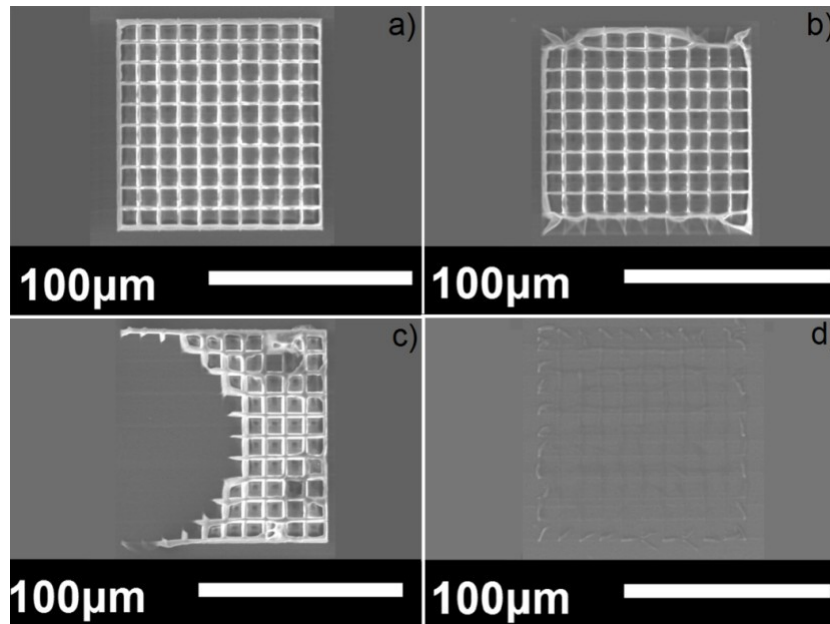


Figure 5: Lattice structure in OrmoComp®: a) $v = 0.8$ mm/s, $P_{avg} = 86$ mW; b) $v = 1$ mm/s, $P_{avg} = 86$ mW; c) $v = 0.5$ mm/s, $P_{avg} = 105$ mW; d) $v = 0.7$ mm/s, $P_{avg} = 37$ mW.

3.3 Fabrication of a branched hollow fiber with pores

Using proper process parameters from the previous section, a 3.5 mm long and 0.55 mm wide branched hollow fiber was fabricated (Fig. 6). The geometry and size of the produced complex hollow fiber were selected according to existing lab-on-chip devices that require these geometries. The inner diameter (ID) of the fiber was set to 90 μm and the outer diameter (OD) to 150 μm . Two small pores (diameter: 30 μm) were placed on top of both arms of the structure to show the possibility of adding other 3D elements. These pores can, for example, facilitate the diffusion of nutrients through the fiber network to supply cells. Although the initial parameter development produced good results with 86 mW average laser power at writing speeds of 0.8 mm/s (Fig. 5a), cycle time reduction was a critical issue to consider. Therefore, the writing speed was set to 5.0 mm/s at 105 mW average laser power. The photo-polymerized fiber is generated layer by layer with 1.0 μm layer distance (z -direction) and 0.5 μm line width (x - y -plane). Due to the fabrication mechanism of the fiber, i.e. layer-by-layer processing and hatching (alternating filling of each layer), the polymerized material is exposed to the laser beam more frequently than a single line of a lattice structure as shown in Fig. 5. In fact, it is inevitable to polymerize the second layer of the fiber without avoiding the interaction of the laser beam with the first layer. Consequently, “more” material polymerizes which allows a much higher writing speed at slightly higher laser power. Fig. 6a shows a cut-off of a fabricated hollow fiber. Minor distortion is observed on the outside wall, near the opening of the fiber (Fig. 6b). This phenomenon can be explained by the outgassing of the solvent after the post-exposure development which leads to shrinkage as the volume decreases due to lost gases, resulting in stress. Figure 6c shows a close-up of a pore with 28.5 μm diameter. Overall, the geometry and size of the pore is in agreement with the initial CAD design. The difference between produced and designed pore diameter is 5% (28.5 μm vs. 30 μm) which is within the range as specified by the resin manufacturer. Figure 6d shows the fabricated branched hollow fiber of 3.5 mm length. The required process time was approximately 11.5 hours.

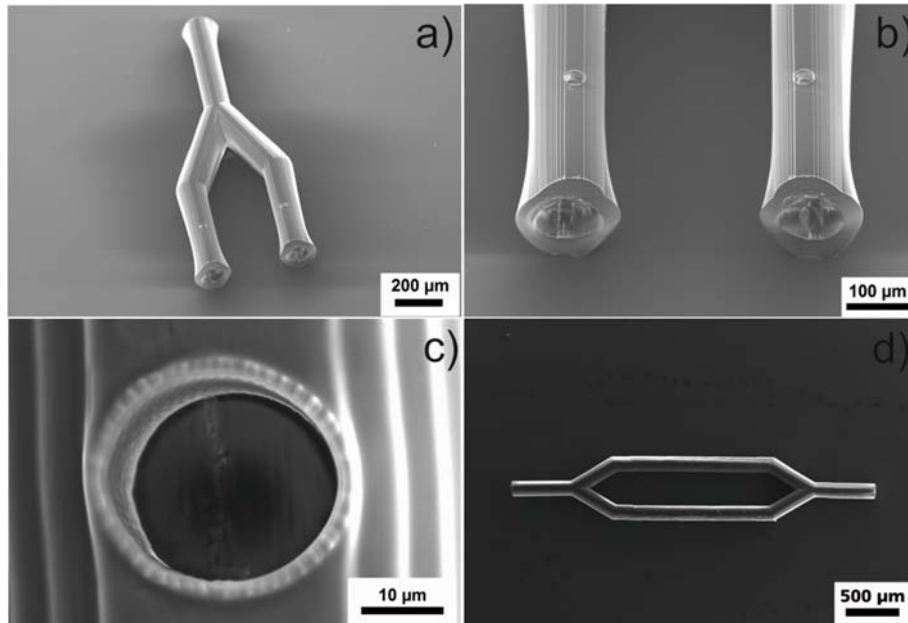


Figure 6: a) Cut-off of a branched hollow fiber fabricated via 2PP of OrmoComp®; b) close-up of the fiber ends; c) pore with 28.5 μm diameter; d) completed hollow fiber: average laser power = 105 mW, writing speed = 5.0 mm/s, length = 3.5 mm, outer diameter = 150 μm , inner diameter = 90 μm .

Images, which were taken with an optical microscope, were used to demonstrate that water flows inside the fabricated branched fiber (Fig. 7). The white arrows in Fig. 7 indicate both direction and position of the fluid at different times along the fiber core. The images shown from Fig. 7a -7d are the evidence of the hollow core.

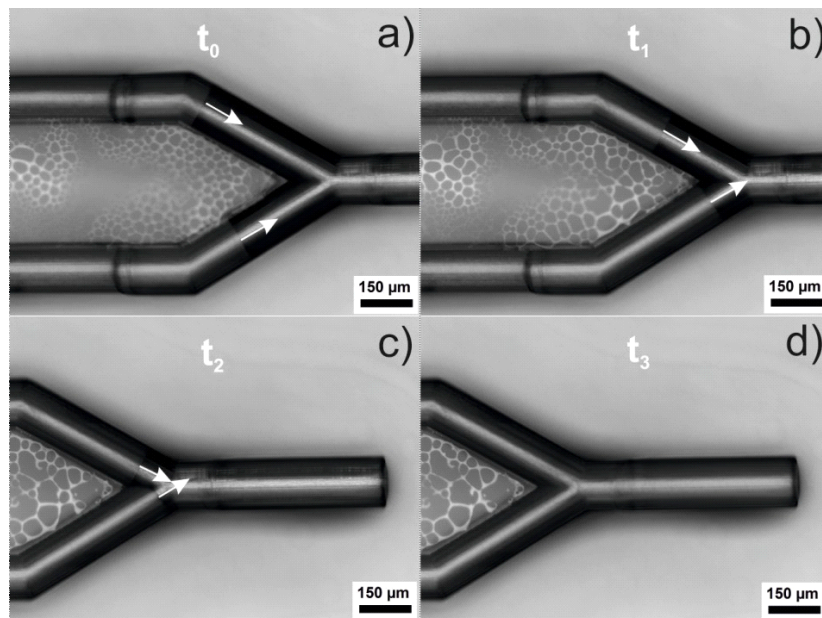


Figure 7: a) – d): Water flowing through the hollow core of a 2PP-fabricated fiber (each picture was taken at a different time t_0 , t_1 , t_2 , and t_3). The arrows indicate both direction and the current position of the water. The time difference between t_0 and t_3 was approximately 25 seconds.

4. Conclusions

Two-photon polymerization provides the ability to generate 3D structures by moving the focal point according to a pre-programmed pattern in an UV curing photoresist. The direct-writing

laser process was employed to fabricate a 3.5 mm long branched hollow fiber (OD: 150 μm , ID: 90 μm) with predefined pores (diameter: 30 μm) in the photoresist OrmoComp®. The required process time was approximately 11.5 hours. The utilized resin could easily be cured without creating too much stress or shrinkage. Acceptable geometrical deviations are in the order of 5 %. The ascending scan method was used to determine the spatial and longitudinal resolution of single voxels upon laser exposure. The smallest lateral width of an isolated voxel was 0.6 μm with a length of 2.6 μm . A variety of lattice-like structures (100 μm x 100 μm) were produced to determine the proper relationship between laser parameters, and writing speed. Well defined lattice structures were obtained at an average laser power of 82 mW and a writing speed of 0.8 mm/s. No polymerization occurred, if the average laser power was too low ($P_{\text{avg}} = 37$ mW at $v = 0.7$ mm/s). Lattice structures with suspended walls showed deformations at an improper exposure ($P_{\text{avg}} = 86$ mW at $v = 1$ mm/s). Structures fabricated above the damage intensity ($P_{\text{avg}} = 105$ mW at $v = 0.5$ mm/s) were boiled, which results in voids and microexplosions, leaving incomplete pattern. The fiber was generated at an average power of 105 mW and a writing speed of 5.0 mm/s. The 2PP-method was proven to be suitable to generate hollow fiber-like structures by successfully passing water through the hollow fiber core after the fabrication process.

Acknowledgements

This work was financially supported by the Fraunhofer Gesellschaft under Grant No. Attract 692174. The Berthold Leibinger Stiftung GmbH is also acknowledged for financial support (Grant No. 149047).

References

- [1] J. Torgersen, A. Baudrimont, N. Pucher, K. Stadlmann, K. Cicha, C. Heller, R. Liska, J. Stampfl, "In Vivo Writing using Two-Photon-Polymerization", *Proceedings of LPM 2010 – The 11th International Symposium on Laser Precision Microfabrication*.
- [2] T. Weiß, R. Schade, T. Laube, A. Berg, G. Hildebrand, R. Wyrwa, M. Schnabelrauch, K. Liefeth, "Two-Photon Polymerization of Biocompatible Photopolymers for Microstructured 3D Biointerfaces", *Advanced Engineering Materials* 2011, 13, No. 9., pp. 264-273.
- [3] M. T. Raimondi, S. M. Eaton, M. Laganà, V. Aprile, M. M. Nava, G. Cerullo, R. Osellame, "Three-dimensional structural niches engineered via two-photon laser polymerization promote stem cell homing", *Acta Biomaterialia* 2013, 9, No. 1, pp. 4579-4584.
- [4] J. Torgersen, A. Ovsianikov, V. Mironov, N. Pucher, X. Qin, Z. Li, K. Cicha, T. Machacek, R. Liska, V. Jantsch, J. Stampfl, "Photo-sensitive hydrogels for threedimensional laser microfabrication in the presence of whole organisms", *Journal of Biomedical Optics* 2012, 17, No.10, pp. 105008.
- [5] E. Käpylä, D. B. Aydogan, S. Virjula, S. Vanhatupa, S. Miettinen, J. Hyttinen, M. Kellomäki, "Direct laser writing and geometrical analysis of scaffolds with designed pore architecture for three-dimensional cell culturing", *Journal of Micromechanics and Microengineering* 2012, 22, pp. 115016.
- [6] A. Koroleva, A. A. Gill, I. Ortega, J. W. Haycock, S. Schlie, S. D. Gittard, B. N. Chichkov, F. Claeysens, "Two-photon polymerization-generated and micromolding-replicated 3D scaffolds for peripheral neural tissue engineering applications", *Biofabrication* 2012, 4, pp. 025005.
- [7] P. Tayalia, C. R. Mendonca, T. Baldacchini, D. J. Mooney, E. Mazur, "3D Cell-Migration Studies using Two-Photon Engineered Polymer Scaffolds", *Advanced Material* 2008, 20, pp. 4494–4498.

- [8] A. Ovsianikov, M. Malinauskas, S. Schlie, B. Chichkov, S. Gittard, R. Narayan, M. Löbler, K. Sternberg, K.-P. Schmitz, A. Haverich, "Three-dimensional laser micro- and nanostructuring of acrylated polyethylene glycol materials and evaluation of their cytotoxicity for tissue engineering applications", *Acta Biomaterial* 2011, 7, No. 3, pp. 967–974.
- [9] A. Nguyen, S.D. Gittard, A. Koroleva, S. Schlie, A. Gaidukeviciute, B. Chichkov, R. Narayan, "Two-photon polymerisation of polyethylene glycol diacrylate scaffolds with riboflavin and triethanolamine used as a water-soluble photoinitiator", *Regenerative Medicine* 2013, 8, No. 6, pp. 725-738.
- [10] G. Cojoc, C. Liberale, P. Candeloro, F. Gentile, G. Das, F. De Angelis, E. Di Fabrizio, "Optical micro-structures fabricated on top of optical fibers by means of two-photon photopolymerization", *Microelectronic Engineering* 2010, 87, pp. 876–879.
- [11] C. Reinhardt, S. Passinger, B. N. Chichkov, C. Marquart, I. P. Radko, S. I. Bozhevolnyi, "Laser-fabricated dielectric optical components for surface plasmon polaritons", *Optics Letters* 2006, 31, No. 9, pp. 1307-1309.
- [12] S. D. Gittard, A. Nguyen, K. Obata, A. Koroleva, R. J. Narayan, B. N. Chichkov, "Fabrication of microscale medical devices by two-photon polymerization with multiple foci via a spatial light modulator", *Biomedical Optics Express* 2011, 2, No. 11, pp. 3167-3178.
- [13] S. D. Gittard, A. Ovsianikov, N. A. Monteiro-Riviere, J. Lusk, P. Morel, P. Minghetti, C. Lenardi, B. N. Chichkov, R. J. Narayan, "Fabrication of Polymer Microneedles Using a Two-Photon Polymerization and Micromolding Process", *Journal of Diabetes Science and Technology* 2009, 3, No. 2, pp. 304-311.
- [14] M. Al-Abaddi, L. Sasso, M. Dimaki, W. E. Svendsen, "Fabrication of 3D nano/microelectrodes via two-photon-polymerization", *Microelectronic Engineering* 2012, 98, pp. 378–381.
- [15] K. Cicha, T. Koch, J. Torgersen, Z. Li, R. Liska, "Young's modulus measurement of two-photon polymerized microcantilevers by using nanoindentation equipment", *Journal of Applied Physics* 2012, 112, pp. 094906.
- [16] M. Göppert-Mayer, "Über Elementarakte mit zwei Quantensprüngen", *Annalen der Physik* 1931, 401, No. 3, pp. 273–294.
- [17] W. Kaiser, C. G. B. Garrett, "Two-Photon Excitation $\text{CaF}_2:\text{Eu}^{2+}$ ", *Physical Review Letters* 1961, 7, No. 6, pp. 229-231.
- [18] H.-B. Sun, S. Kawata, "Two-Photon Photopolymerization and 3D Lithographic Microfabrication" in *NMR • 3D Analysis • Photopolymerization*, Volume 170 of the series *Advances in Polymer Science* 2006, pp 169-273, Springer-Verlag Berlin Heidelberg.
- [19] M. Pawlicki, H. A. Collins, R. G. Denning, H. L. Anderson, "Two-Photon Absorption and the Design of Two-Photon Dyes", *Angewandte Chemie International Edition* 2009, 48, pp. 3244 – 3266.
- [20] K. Sugioka, Y. Cheng, "Femtosecond laser three-dimensional micro- and nanofabrication", *Applied Physics Reviews* 2014, 1, pp. 041303.
- [21] K. H. Lee, S. J. Shin, Y. Park, S.-H. Lee, "Synthesis of Cell-Laden Alginate Hollow Fibers Using Microfluidic Chips and Microvascularized Tissue-Engineering Applications", *small* 2009, 5, No. 11, pp. 1264–1268.

- [22] Y. Kitagawa, M. Yamada, M. Seki, "Microengineered Hydrogel Fibers for Evaluating Cancer Cell Invasion under 3D Coculture Conditions", *17th International Conference on Miniaturized Systems for Chemistry and Life Sciences 2013*.
- [23] H. Onoe, T. Okitsu, A. Itou, M. Kato-Negishi, R. Gojo, D. Kiriya, K. Sato, S. Miura, S. Iwanaga, K. Kuribayashi-Shigetomi, Y. T. Matsunaga, Y. Shimoyama, S. Takeuchi, "Metre-long cell-laden microfibres exhibit tissue morphologies and functions", *Nature Materials* 2013, 12, pp. 584-590.
- [24] Q. Z. Yu, Y. M. Qin, "Fabrication and formation mechanism of poly(L-lactic acid) ultrafine multi-porous hollow fiber by electrospinning", *eXPRESS Polymer Letters* 2013, 7, No.1, pp. 55–62.
- [25] G. Kumi, C. O. Yanez, K. D. Belfield, J. T. Fourkas, "High-speed multiphoton absorption polymerization: fabrication of microfluidic channels with arbitrary cross-sections and high aspect ratios", *Lab Chip* 2010, 10, pp. 1057-1060.
- [26] K. Venkatakrisnan, S. Jariwala, B. Tan, „Maskless fabrication of nano-fluidic channels by two-photon absorption (TPA) polymerization of SU-8 on glass substrate", *Optics Express* 2009, 17, 4, pp. 2756-2762.
- [27] S. Jariwala, K. Venkatakrisnan, B. Tan, „Single step self-enclosed fluidic channels via two photon absorption (TPA) polymerization", *Optics Express* 2010, 18, 2, pp. 1630-1636.
- [28] H.-B. Sun, T. Tanaka, S. Kawata, "Three-dimensional focal spots related to two-photon excitation", *Applied Physics Letters* 2002, 80, No. 20, pp. 3673-3675.
- [29] M. Farsari, G. Filippidis, C. Fotakis, "Fabrication of three-dimensional structures by three-photon polymerization", *Optics Letters* 2005, 30, No. 23, pp. 3180-3182.
- [30] C.R. Mendonca, D.S. Correa, T. Baldacchini, P. Tayalia, E. Mazur, "Two-photon absorption spectrum of the photoinitiator Lucirin TPO-L", *Applied Physics A* 2008, 90, pp.633–636.